Supplement of Hydrol. Earth Syst. Sci., 28, 1827–1851, 2024
https://doi.org/10.5194/hess-28-1827-2024-supplement

Hydrology and Earth System Sciences
Open Access
EGU

Supplement of

Unraveling phenological and stomatal responses to flash drought and implications for water and carbon budgets

Nicholas K. Corak et al.

Correspondence to: Lauren E. L. Lowman (lowmanle@wfu.edu)

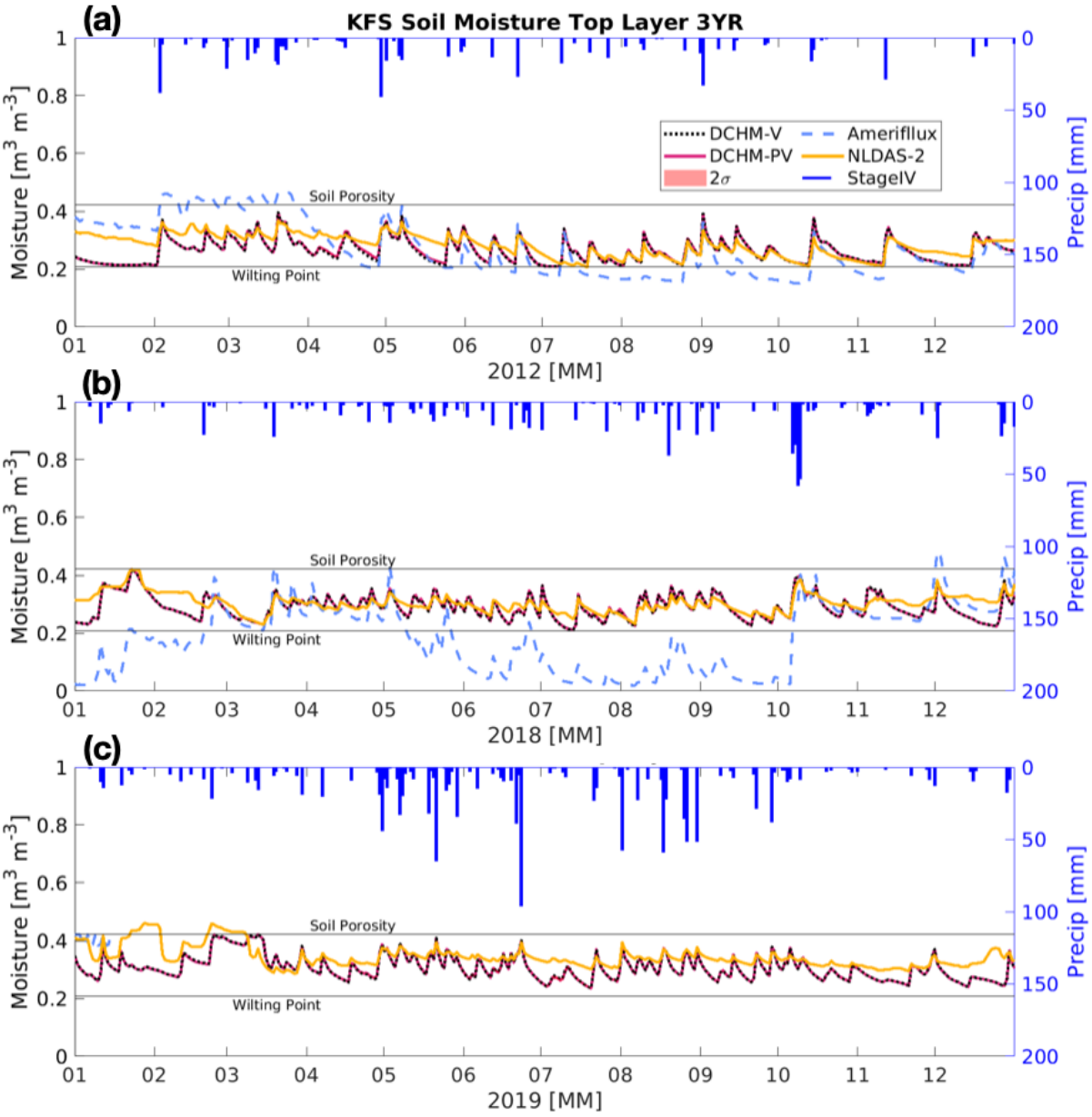

Figure S1. Top layer soil moisture at US-KFS for (a) 2012, flash drought, (b) 2018 drought and (c) 2019 a non-drought year using the DCHM-V (black dotted line), the DCHM-PV with two standard deviations (red), AmeriFlux (blue dashed line), NLDAS-2 derived from Noah-LSM (yellow) and Stage IV precipitation on the top and right axes (blue).

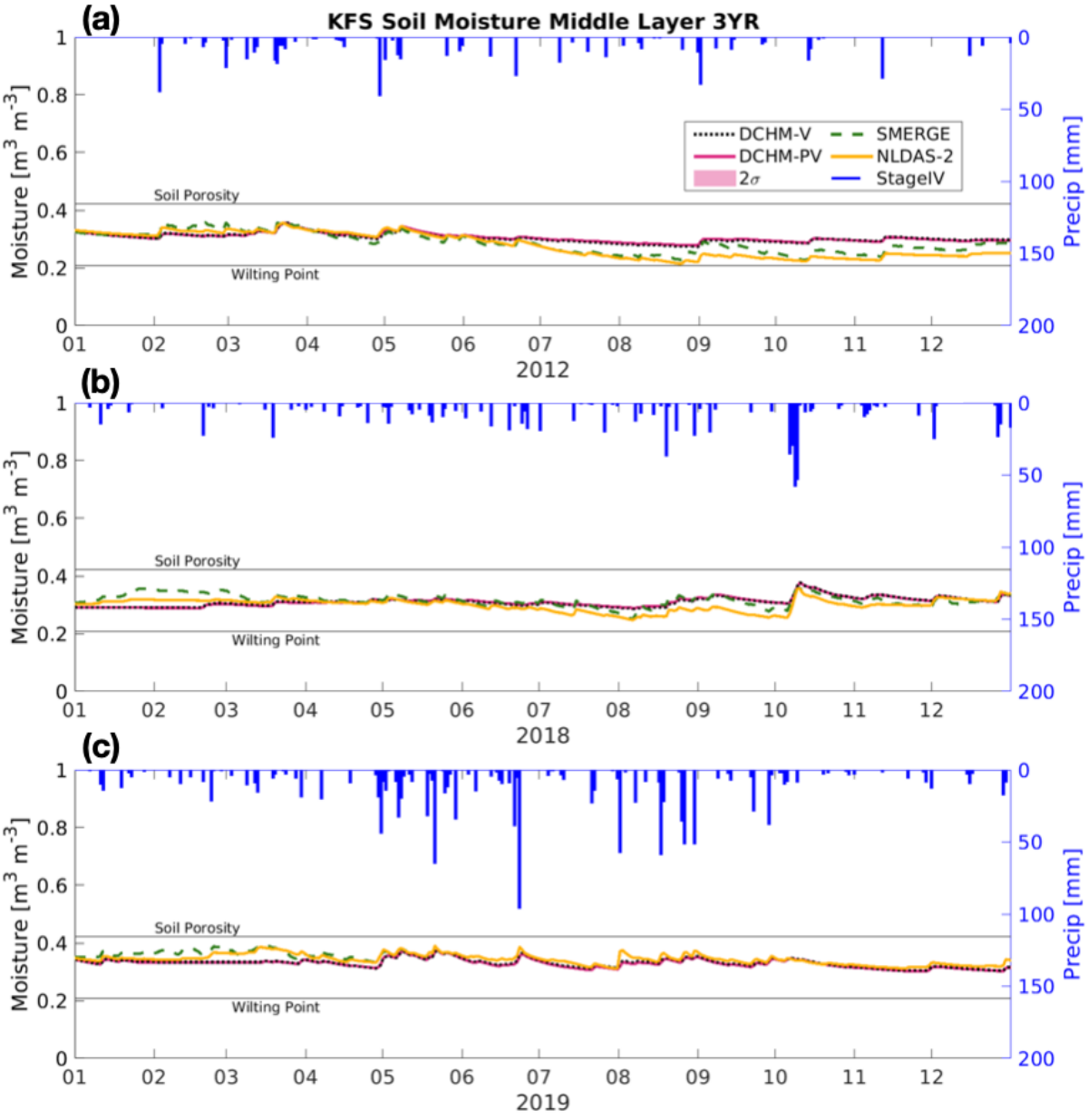

Figure S2. Middle soil moisture at US-KFS for (a) 2012, flash drought, (b) 2018 drought and (c) 2019 a non-drought year using the DCHM-V (black dotted line), the DCHM-PV with two standard deviations (red), AmeriFlux (blue dashed line), NLDAS-2 derived from Noah-LSM (yellow) and Stage IV precipitation on the top and right axes (blue).

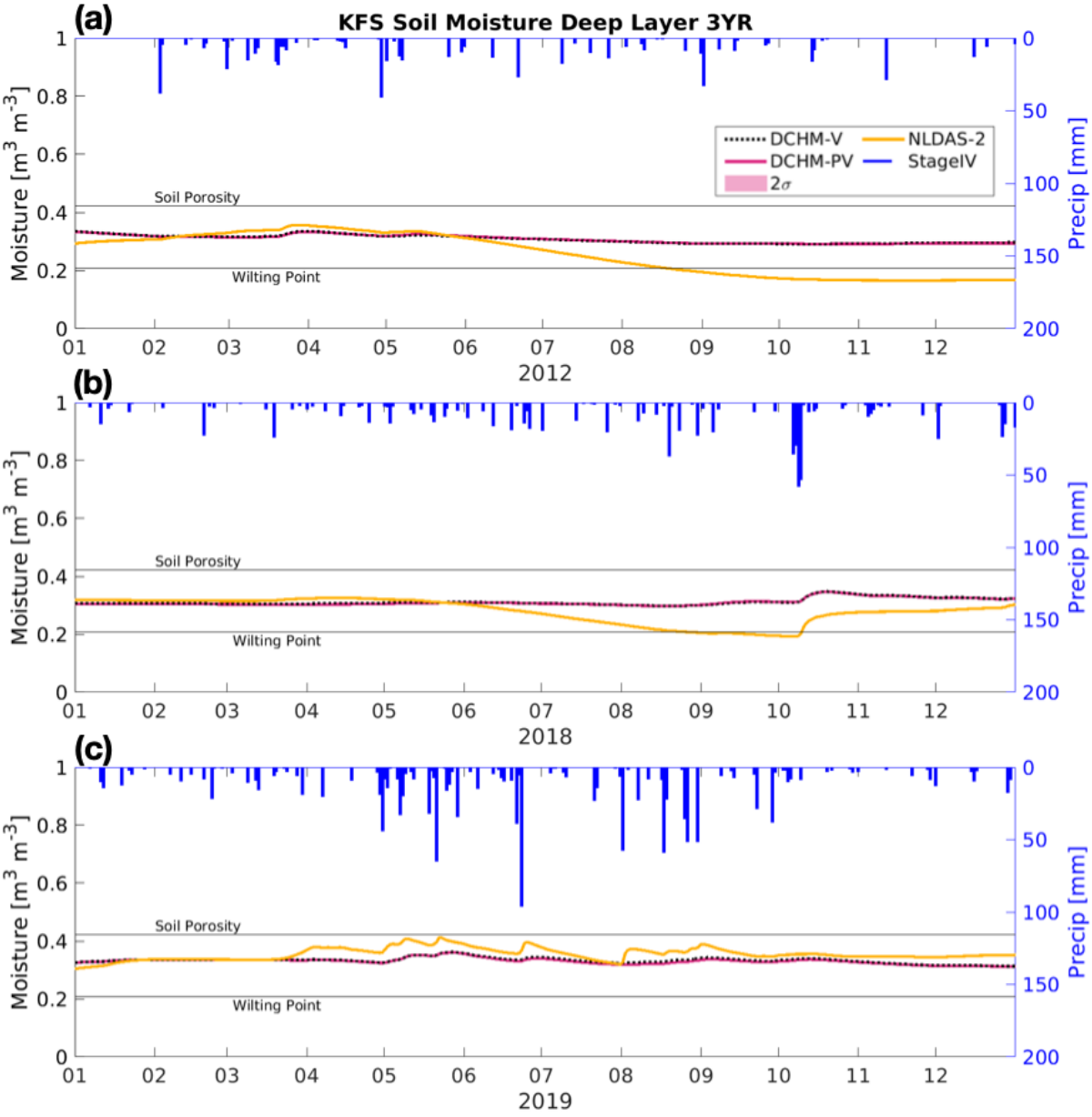

Figure S3. Deep soil moisture at US-KFS for (a) 2012, flash drought, (b) 2018 drought and (c) 2019 a non-drought year using the DCHM-V (black dotted line), the DCHM-PV with two standard deviations (red), AmeriFlux (blue dashed line), NLDAS-2 derived from Noah-LSM (yellow) and Stage IV precipitation on the top and right axes (blue).

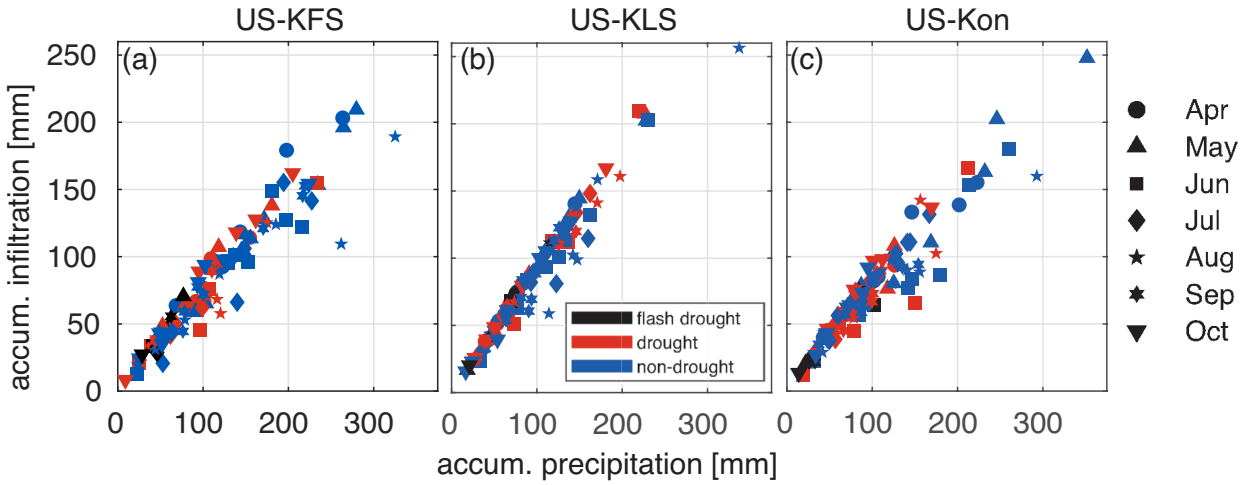

Figure S4. Monthly accumulation of infiltration versus precipitation. Each shape indicates one month over which the averaging occurred and colors distinguish flash drought (black) from drought (red) and non-drought years (blue).

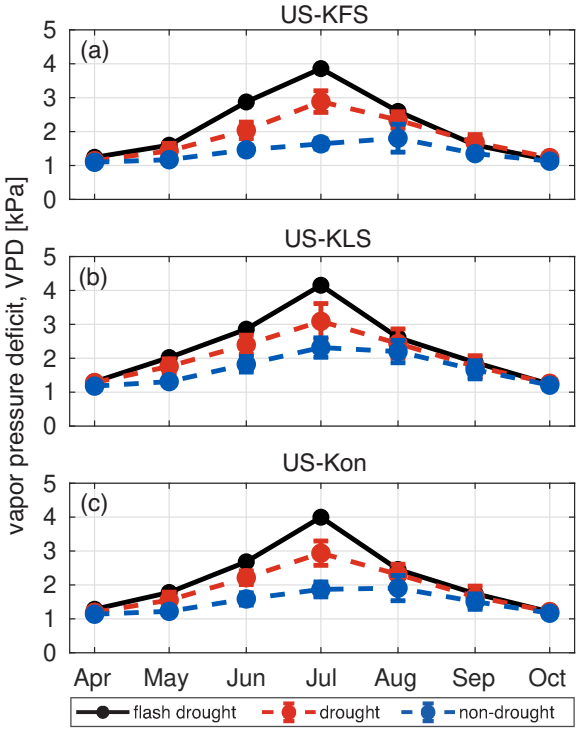

Figure S5. Monthly average vapor pressure deficit [kPa] for the three AmeriFlux sites from April - October for the flash drought year 2012 (black), drought (red), and non-drought (blue). The error bar represents one standard deviation across drought and non-drought years, respectively.

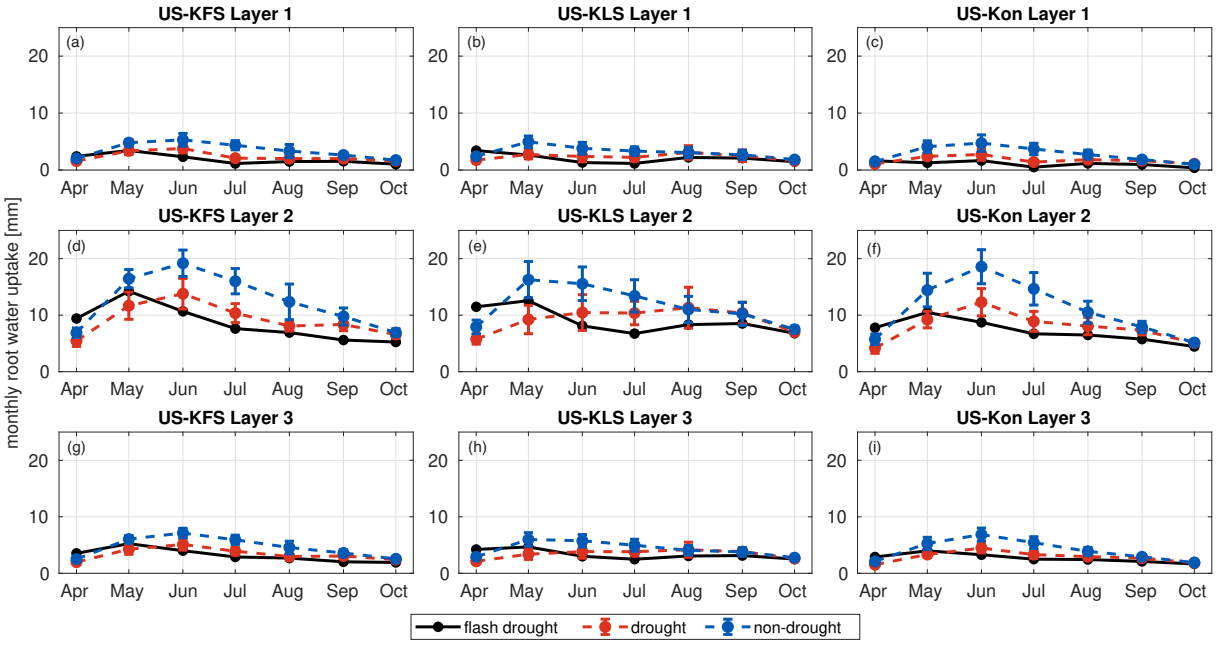

Figure S6. DCHM-PV 3YR monthly root water uptake totals for drought (red) and non-drought (blue) years compared to flash drought (black) across three soil layers for our three study sites. Monthly sums are computed from the ensemble means of the 2000 Monte Carlo simulations then averaged across drought or non-drought years. Error bars represent one standard deviation across drought and non-drought years, respectively.

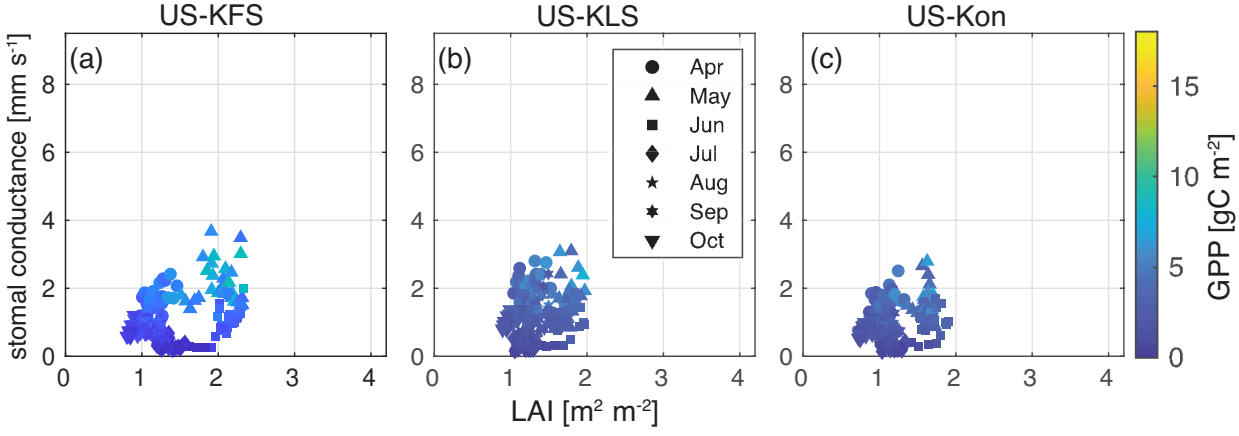

Figure S7. Daily stomatal conductance [mm s^{-1}] vs leaf area index, LAI [m^2 m^{-2}] for all three sites during the flash drought of 2012. Marker shapes indicate individual days from April 1 - October 31 from the selected year. Each month is given a unique shape and daily totals of gross primary productivity [gC m^{-2}] are indicated by color.

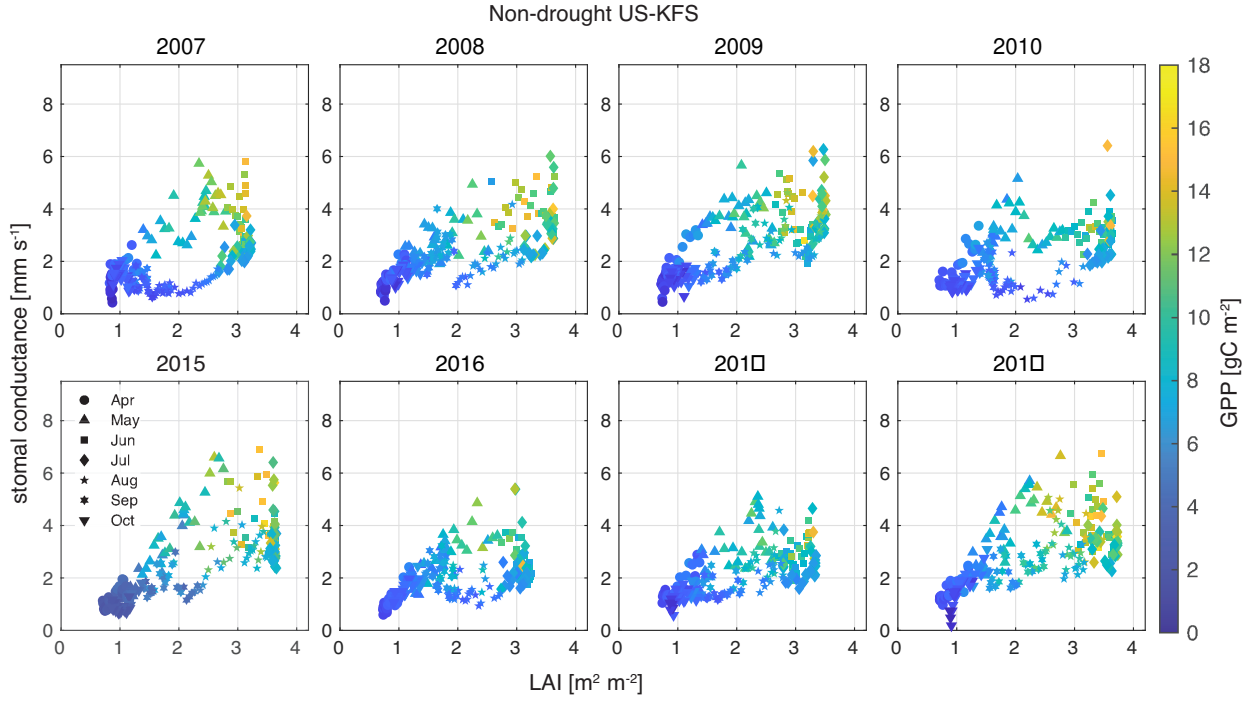

Figure S8. Daily stomatal conductance [mm s^{-1}] vs leaf area index, LAI [m^2 m^{-2}] for US-KFS for selected non-drought years. Marker shapes indicate individual days from April 1 - October 31 from the selected drought year. Each month is given a unique shape and daily totals of gross primary productivity [gC m^{-2}] are indicated by color.

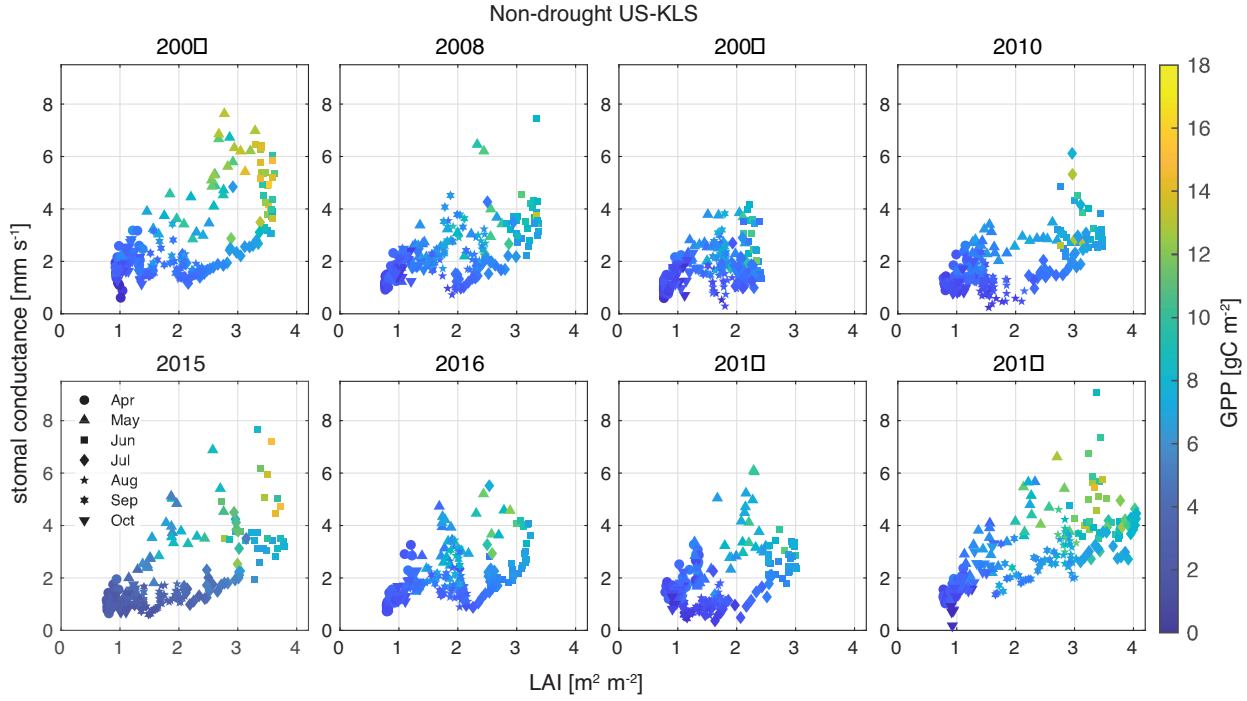

Figure S9. Daily stomatal conductance [mm s^{-1}] vs leaf area index, LAI [m^2 m^{-2}] for US-KLS for selected non-drought years. Marker shapes indicate individual days from April 1 - October 31 from the selected drought year. Each month is given a unique shape and daily totals of gross primary productivity [gC m^{-2}] are indicated by color.

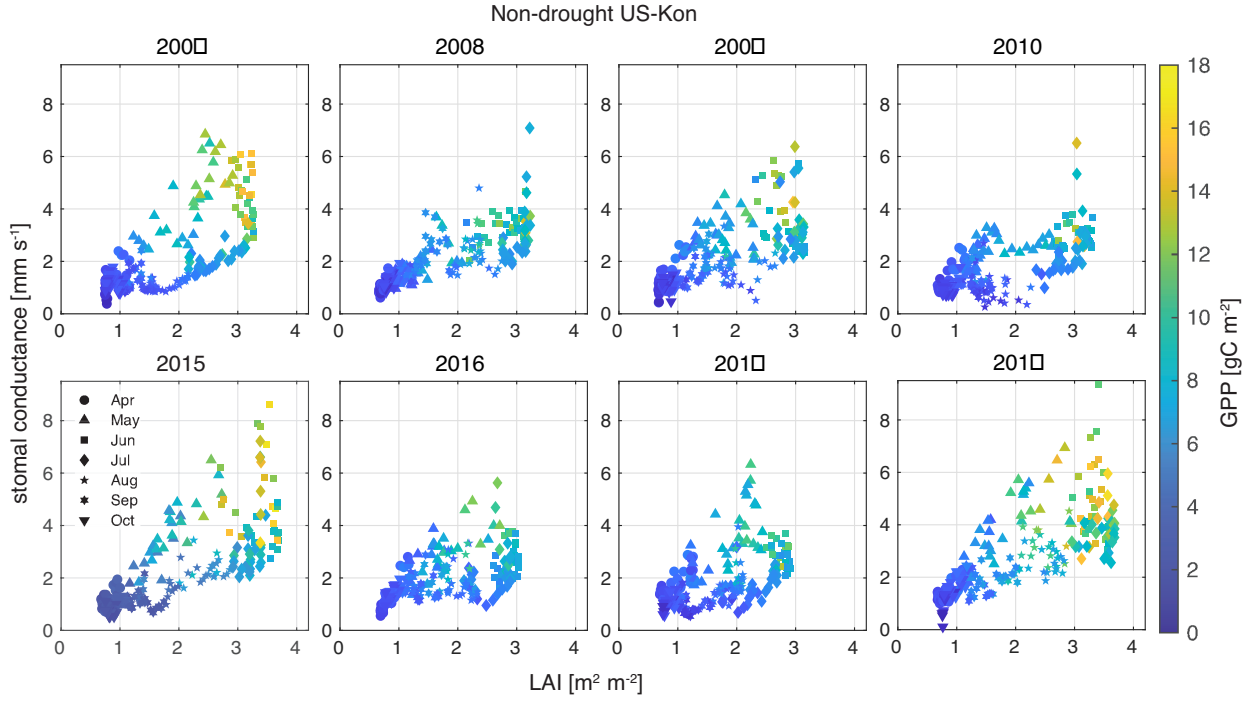

Figure S10. Daily stomatal conductance [mm s^{-1}] vs leaf area index, LAI [m^2 m^{-2}] for US-Kon for selected non-drought years. Marker shapes indicate individual days from April 1 - October 31 from the selected drought year. Each month is given a unique shape and daily totals of gross primary productivity [gC m^{-2}] are indicated by color.

Figure S11. Daily stomatal conductance [mm s^{-1}] vs leaf area index, LAI [m^2 m^{-2}] for all three study sites for selected drought years. Marker shapes indicate individual days from April 1 - October 31 from the selected drought year. Each month is given a unique shape and daily totals of gross primary productivity [gC m^{-2}] are indicated by color.

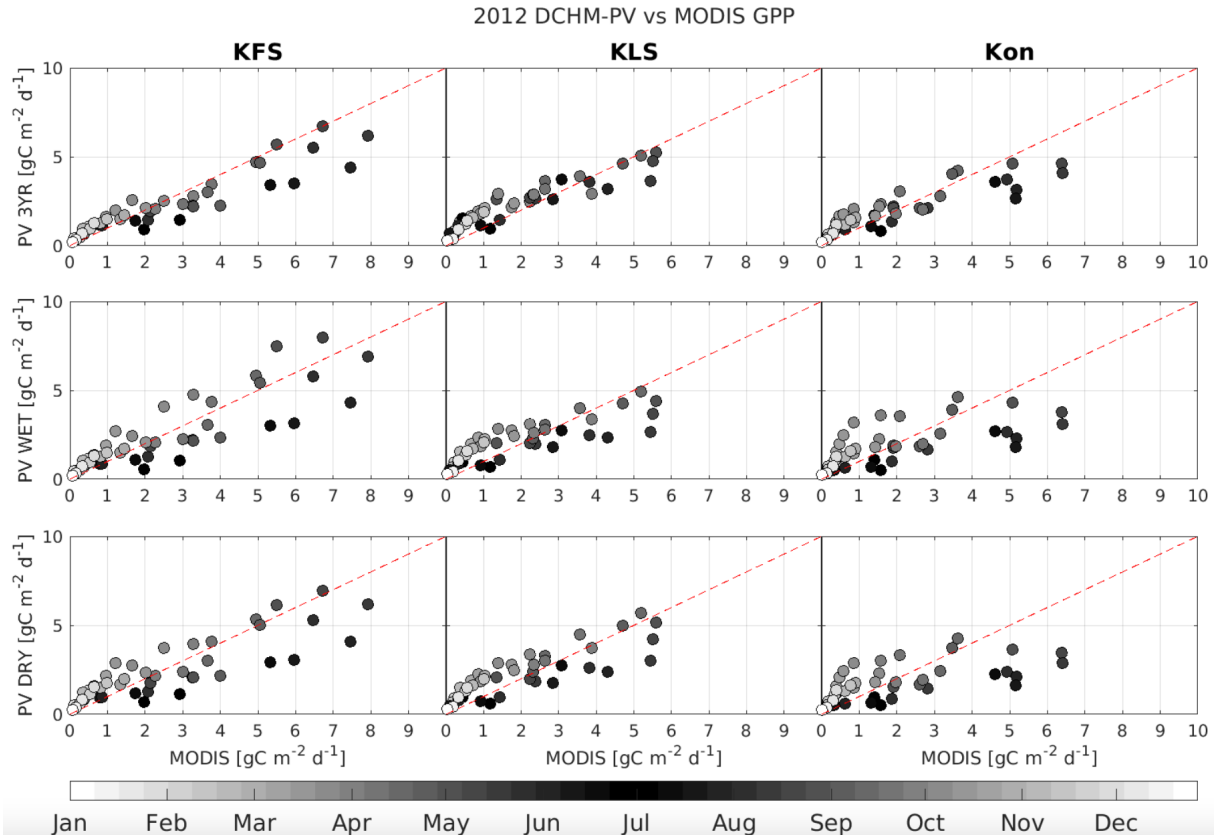

Figure S12. Daily average GPP in 2012 (flash drought year) from MODIS MOD17A2H compared against DCHM-PV 3YR (top row), WET (middle row), and DRY (bottom row) simulations. Points are colored by the month in which they occur. The 1:1 line is displayed in red.

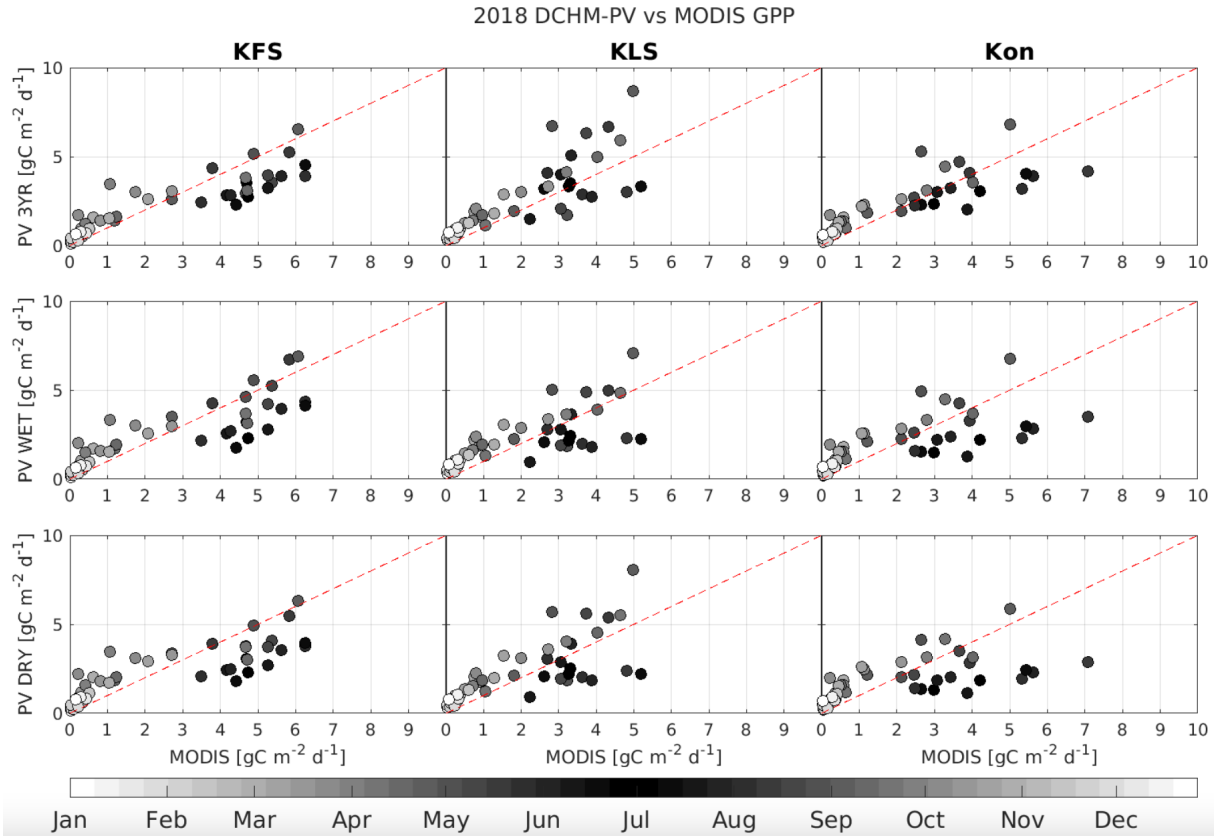

Figure S13. Daily average GPP in 2018 (drought year) from MODIS MOD17A2H compared against DCHM-PV 3YR (top row), WET (middle row), and DRY (bottom row) simulations. Points are colored by the month in which they occur. The 1:1 line is displayed in red.

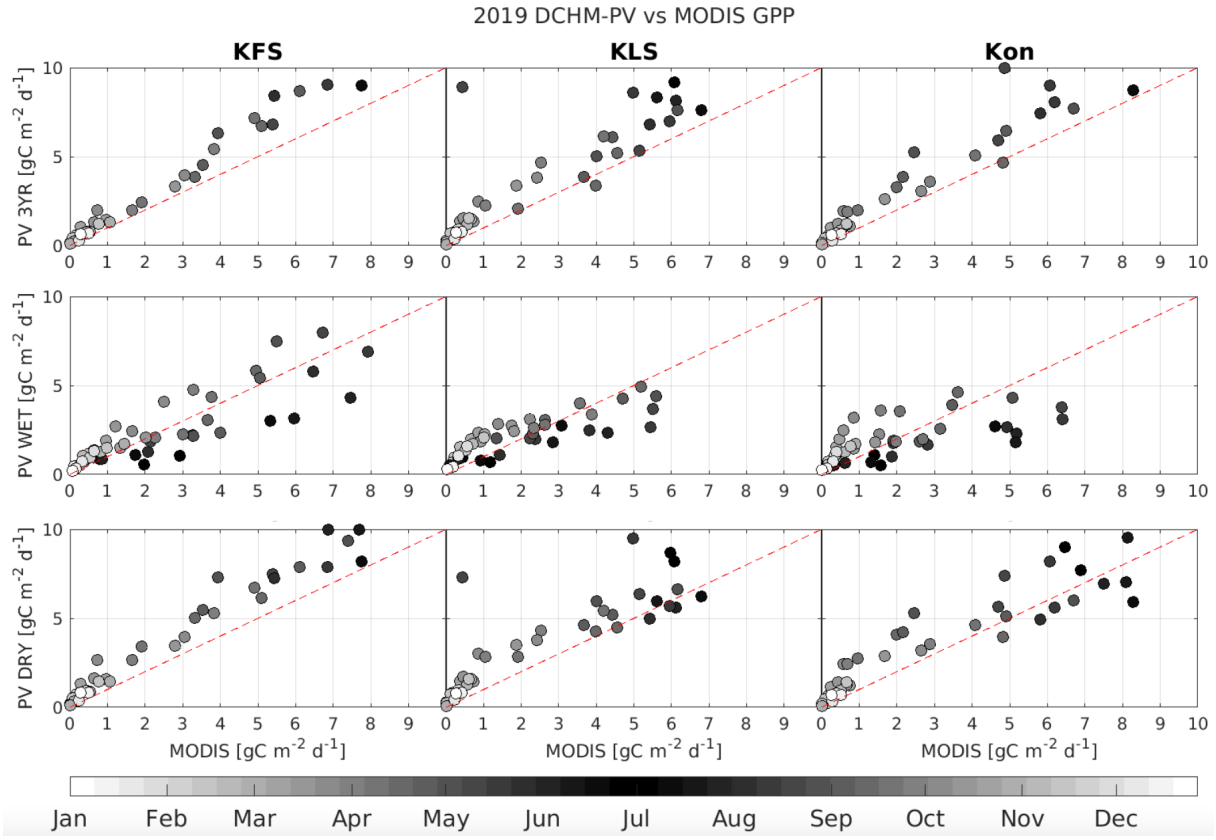

Figure S14. Daily average GPP in 2019 (non-drought year) from MODIS MOD17A2H compared against DCHM-PV 3YR (top row), WET (middle row), and DRY (bottom row) simulations. Points are colored by the month in which they occur. The 1:1 line is displayed in red.

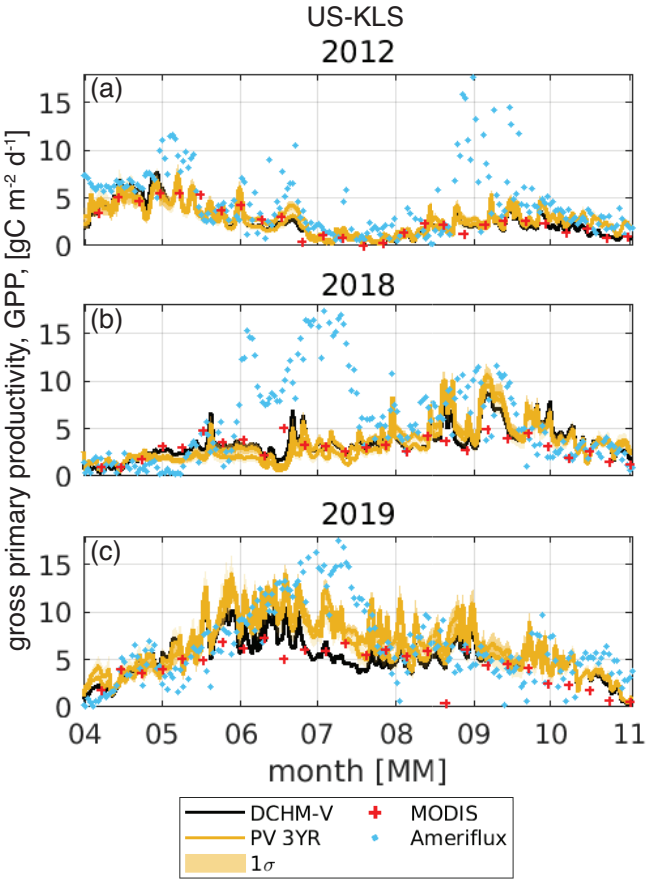

Figure S15. Daily gross primary productivity, GPP, at US-KLS for (a) 2012 flash drought, (b) 2018 drought and (c) 2019 a non-drought year. One standard deviation is shown as a shaded region for the DCHM-PV simulations. MODIS GPP are shown as red crosses and AmeriFlux GPP as blue dots.

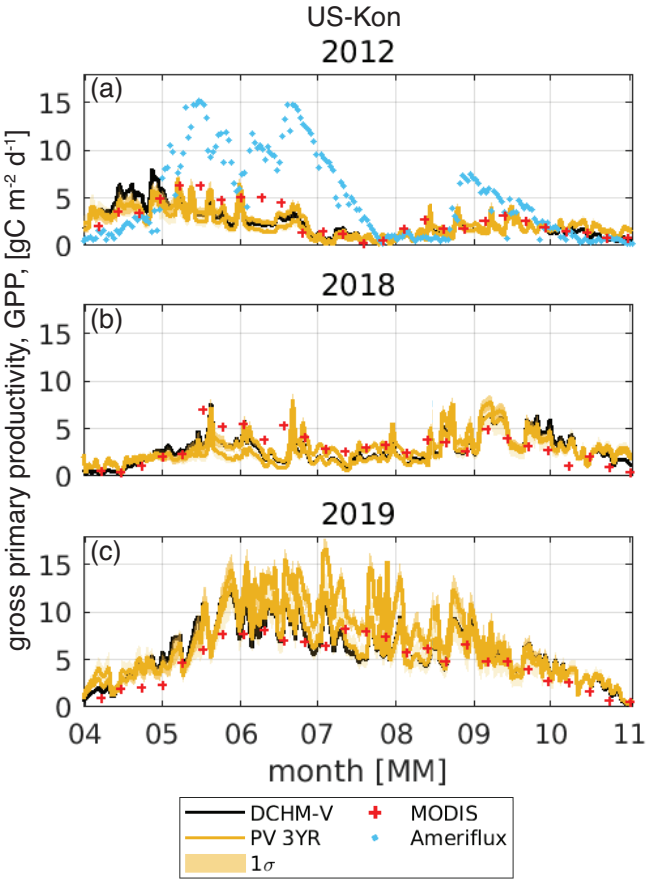

Figure S16. Daily gross primary productivity, GPP, at US-Kon for (a) 2012 flash drought, (b) 2018 drought and (c) 2019 a non-drought year. One standard deviation is shown as a shaded region for the DCHM-PV simulations. MODIS GPP are shown as red crosses and AmeriFlux GPP as blue dots.

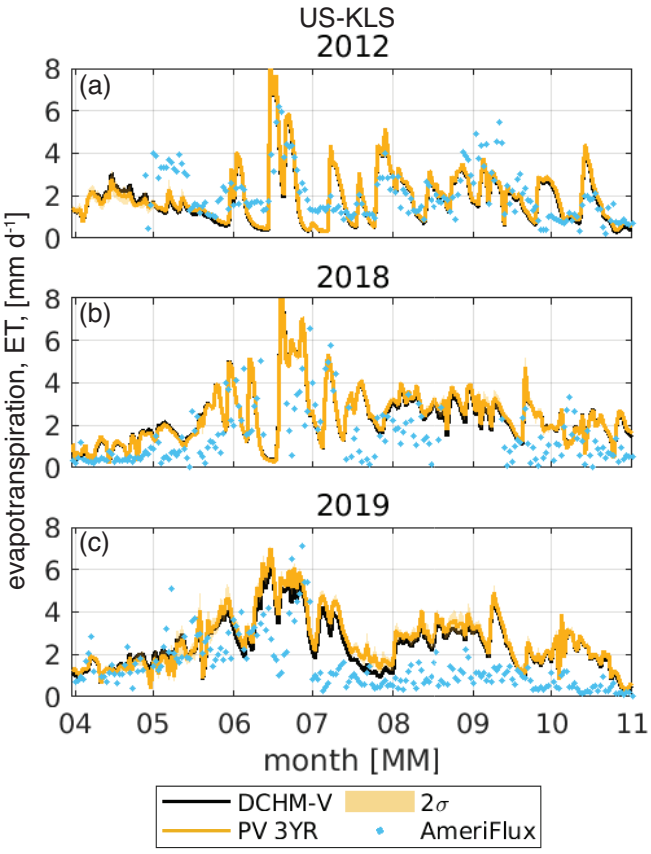

Figure S17. Daily evapotranspiration, ET, at US-KLS for (a) 2012 flash drought, (b) 2018 drought and (c) 2019 a non-drought year. Two standard deviations are shown for the DCHM-PV simulations. AmeriFlux ET is derived from latent heat measurements and shown as blue dots.

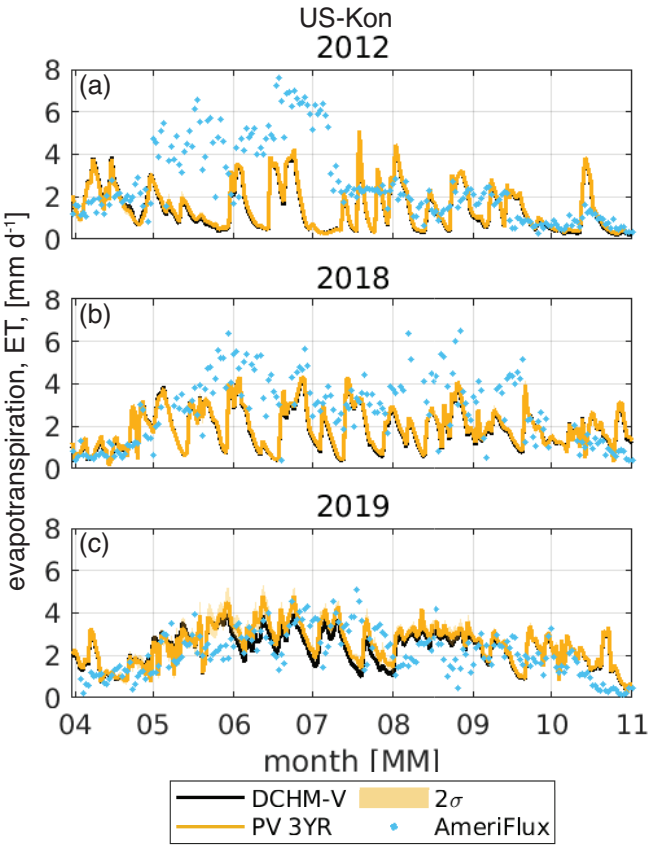

Figure S18. Daily evapotranspiration, ET, at US-Kon for (a) 2012 flash drought, (b) 2018 drought and (c) 2019 a non-drought year. Two standard deviations are shown for the DCHM-PV simulations. AmeriFlux ET is derived from latent heat measurements and shown as blue dots.

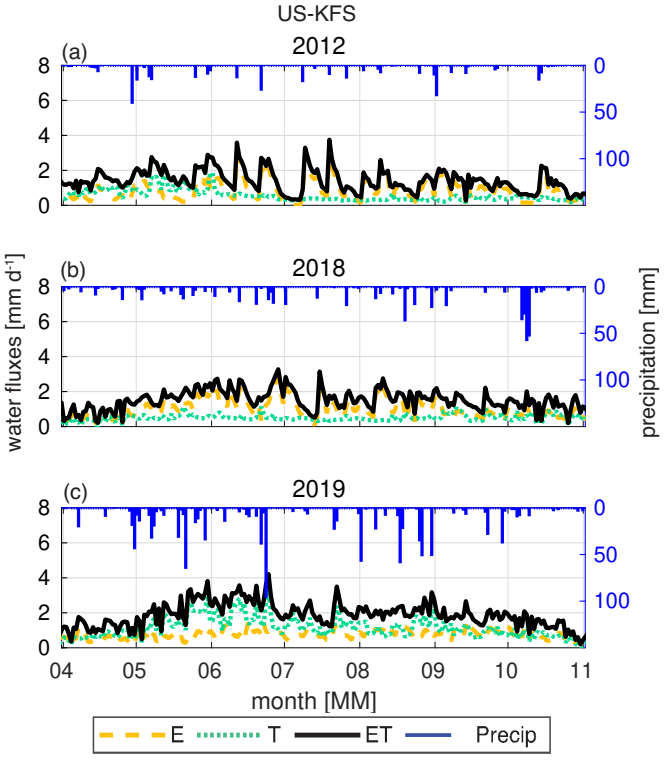

Figure S19. Daily evapotranspiration, ET, partitioned into evaporation, E, and transpiration, T, in mm d^{-1} at US-KFS for (a) 2012 flash drought, (b) 2018 drought, and (c) a 2019 non-drought year. The curves represent ensemble means from the DCHM-PV 3YR. Daily precipitation accumulation is shown on the right axis.

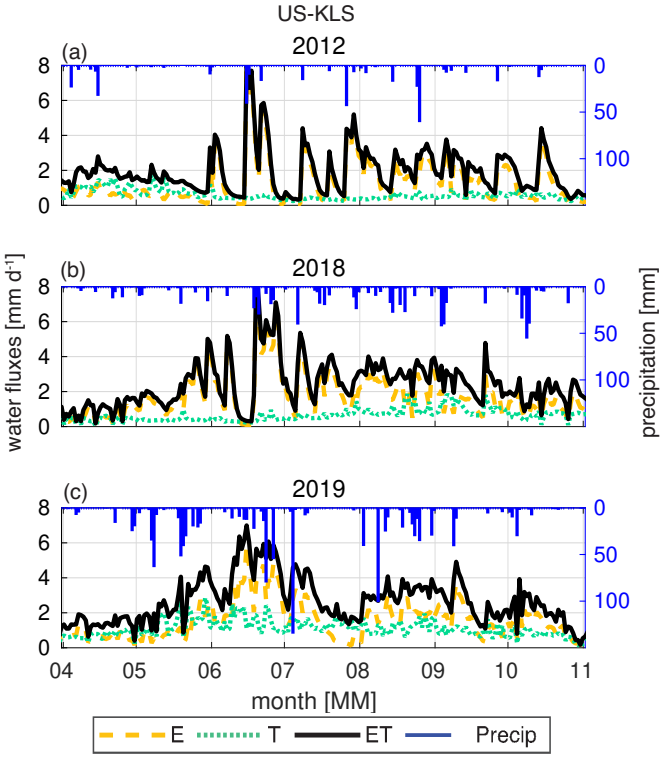

Figure S20. Daily evapotranspiration, ET, partitioned into evaporation, E, and transpiration, T, in mm d^{-1} at US-KLS for (a) 2012 flash drought, (b) 2018 drought, and (c) a 2019 non-drought year. The curves represent ensemble means from the DCHM-PV 3YR. Daily precipitation accumulation is shown on the right axis.

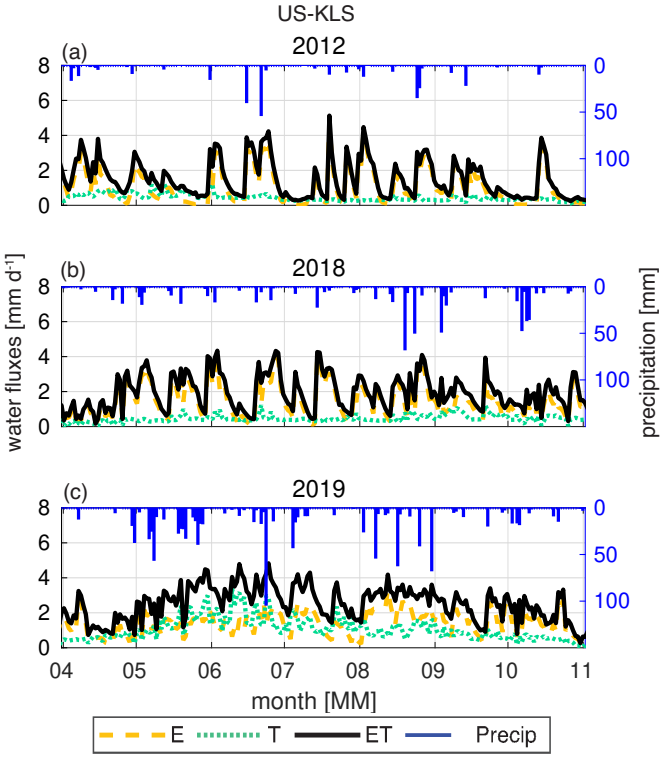

Figure S21. Daily evapotranspiration, ET, partitioned into evaporation, E, and transpiration, T, in mm d^{-1} at US-Kon for (a) 2012 flash drought, (b) 2018 drought, and (c) a 2019 non-drought year. The curves represent ensemble means from the DCHM-PV 3YR. Daily precipitation accumulation is shown on the right axis.

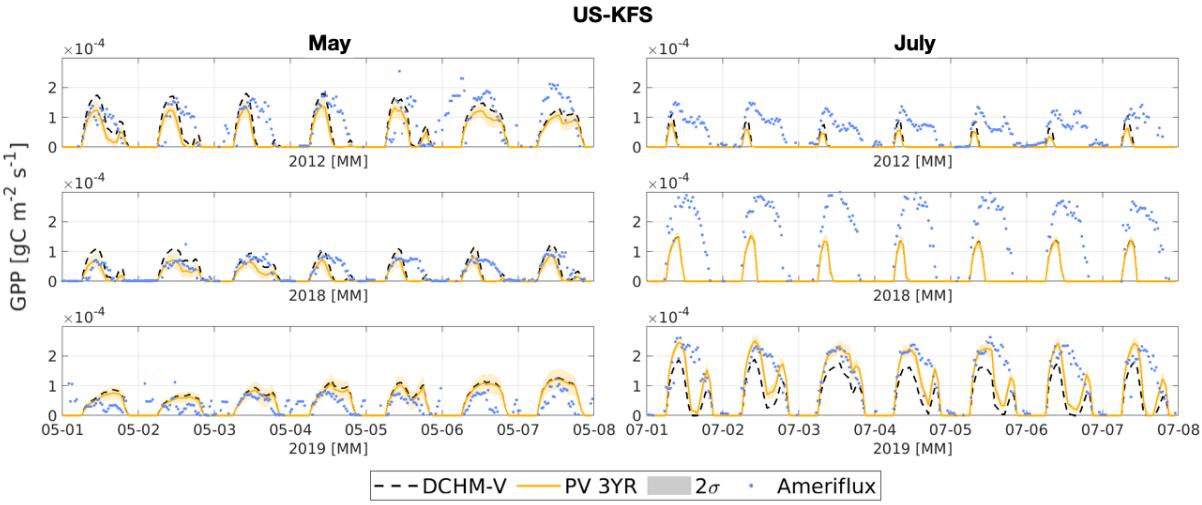

Figure S22. Hourly gross primary productivity [gC m^{-2} s^{-1}] from the DCHM-V and DCHM-PV shown against AmeriFlux 30-minute estimates for one week in May and July of 2012, 2018, and 2019 at US-KFS.

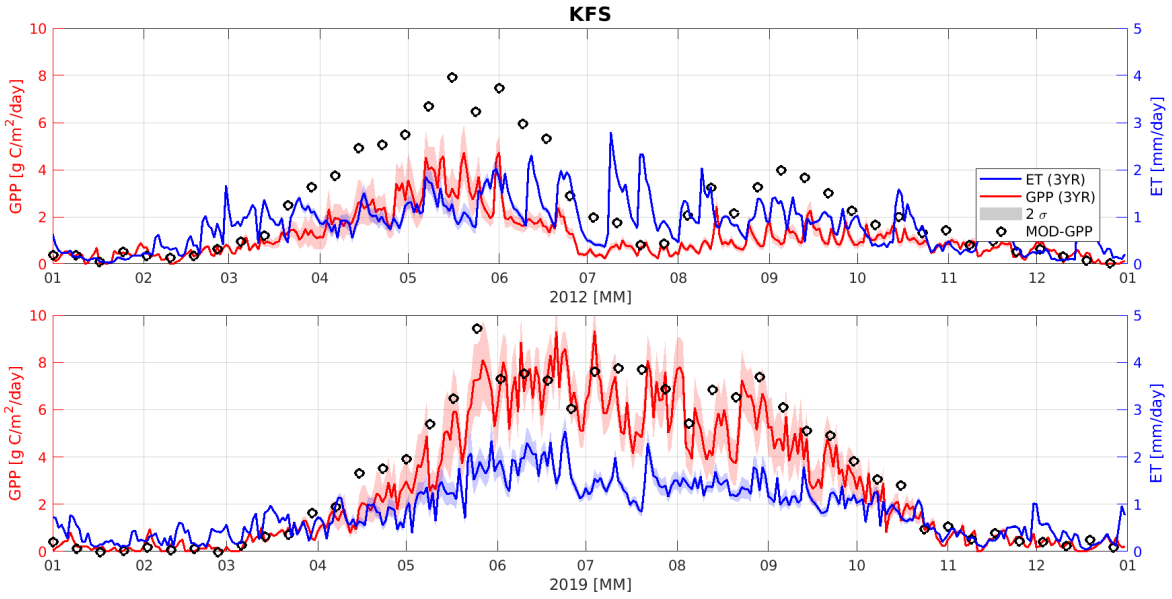

Figure S23. Simulated daily totals of GPP and ET from the DCHM-PV 3YR assimilation period for (a) 2012, flash drought year and (b) 2019, wet year.

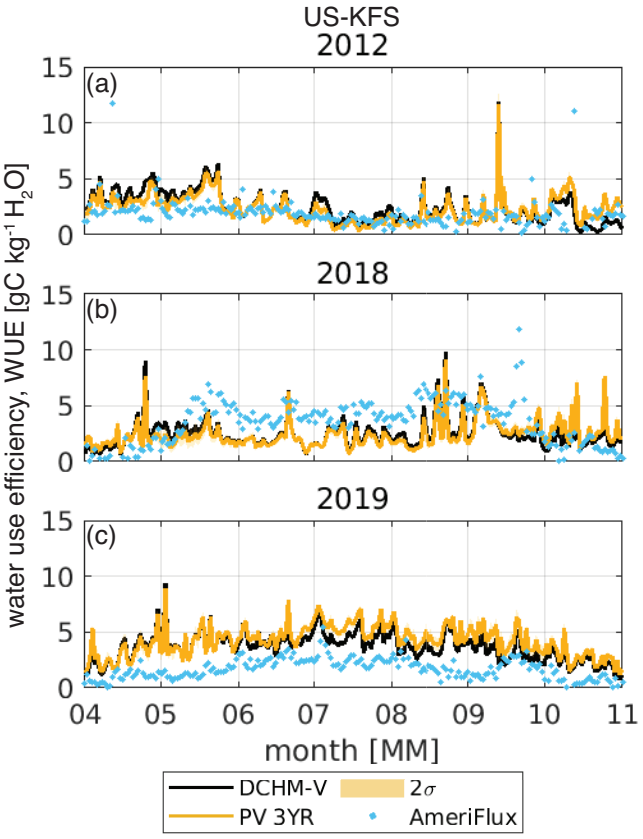

Figure S24. Growing season water-use efficiency (WUE=GPP/ET) from DCHM-V, DCHM-PV (3YR), and AmeriFlux for (a) 2012 flash drought, (b) 2018 drought, and (c) 2019 non-drought at US-KFS. Ensemble means shown for DCHM-PV with 2 standard deviations (shaded).

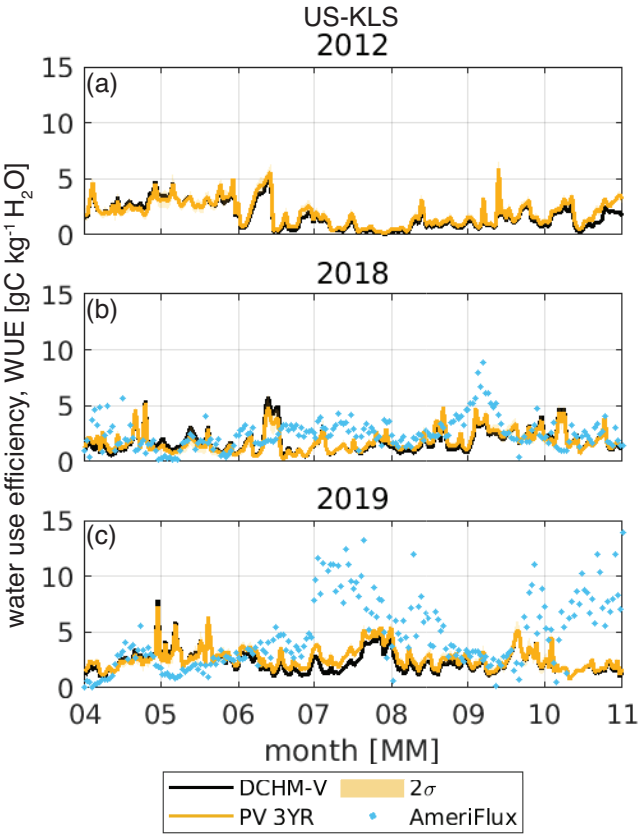

Figure S25. Growing season water-use efficiency (WUE=GPP/ET) from DCHM-V, DCHM-PV (3YR), and AmeriFlux for (a) 2012 flash drought, (b) 2018 drought, and (c) 2019 non-drought at US-KLS. Ensemble means shown for DCHM-PV with 2 standard deviations (shaded).

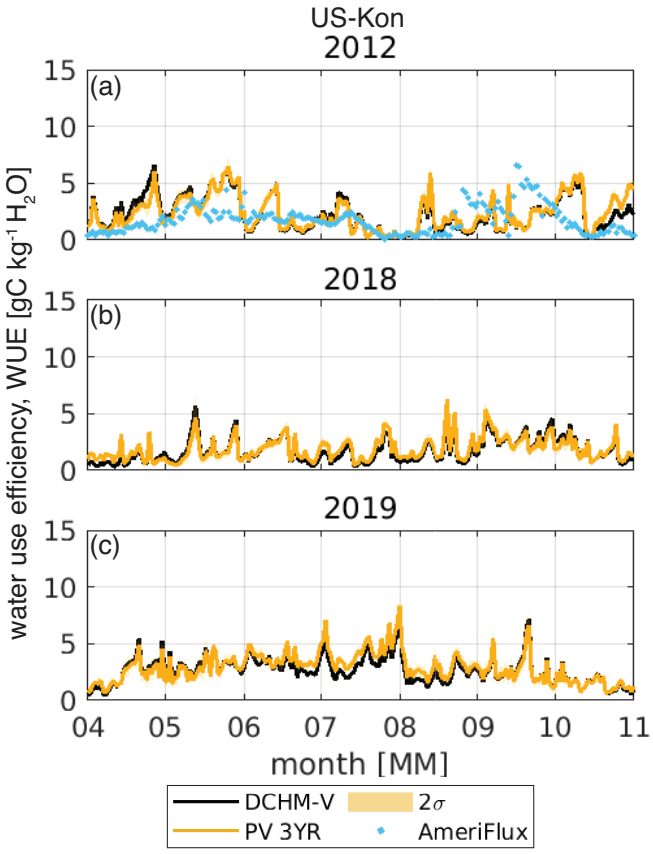

Figure S26. Growing season water-use efficiency (WUE=GPP/ET) from DCHM-V, DCHM-PV (3YR), and AmeriFlux for (a) 2012 flash drought, (b) 2018 drought, and (c) 2019 non-drought at US-Kon. Ensemble means shown for DCHM-PV with 2 standard deviations (shaded).

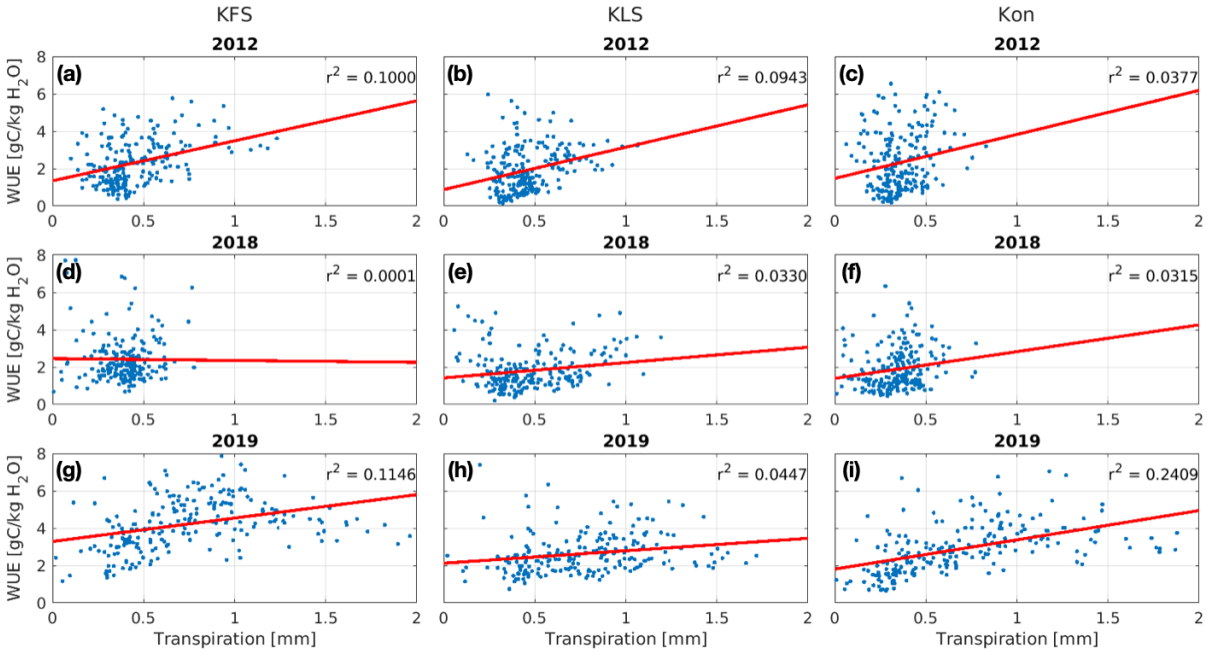

Figure S27. Daily averages of water-use efficiency versus transpiration for 2012, 2018, and 2019.

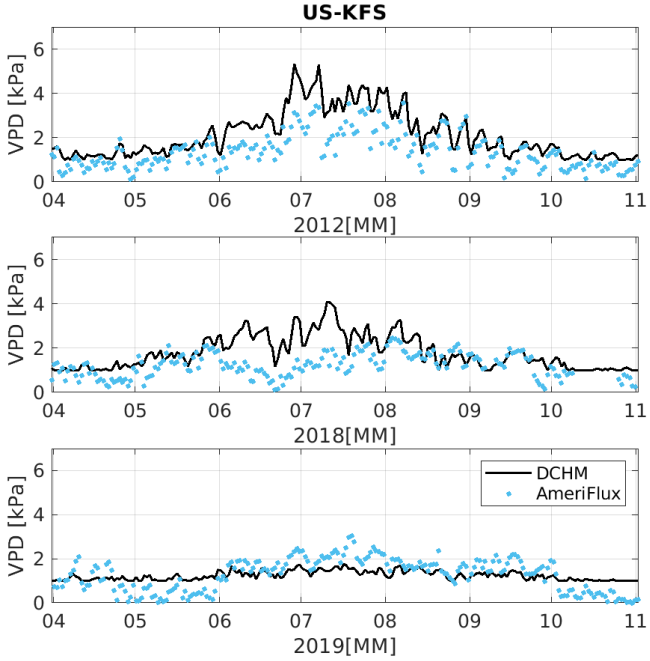

Figure S28. Daily vapor pressure deficit at US-KFS for (a) 2012 - flash drought, (b) 2018 - drought and (c) 2019 - non-drought. The DCHM computes VPD using air temperature and vapor pressure from NLDAS-2 Forcing File A.

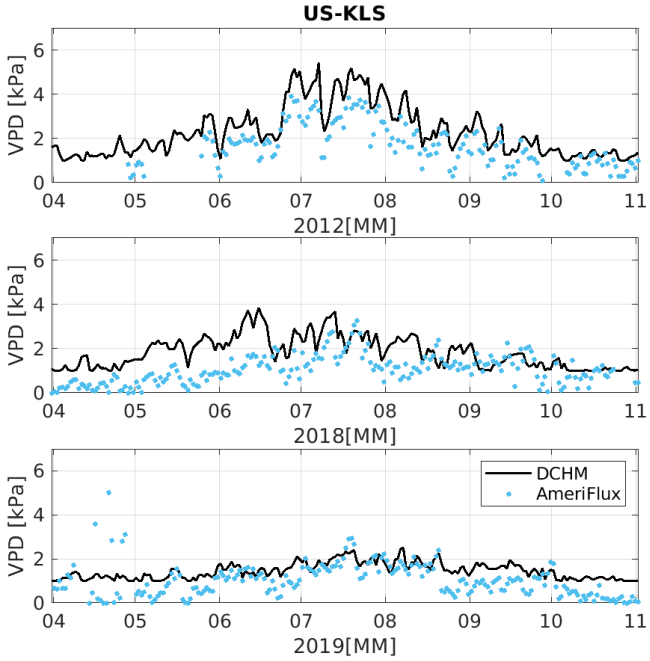

Figure S29. Daily vapor pressure deficit at US-KLS for (a) 2012 - flash drought, (b) 2018 - drought and (c) 2019 - non-drought. The DCHM computes VPD using air temperature and vapor pressure from NLDAS-2 Forcing File A.

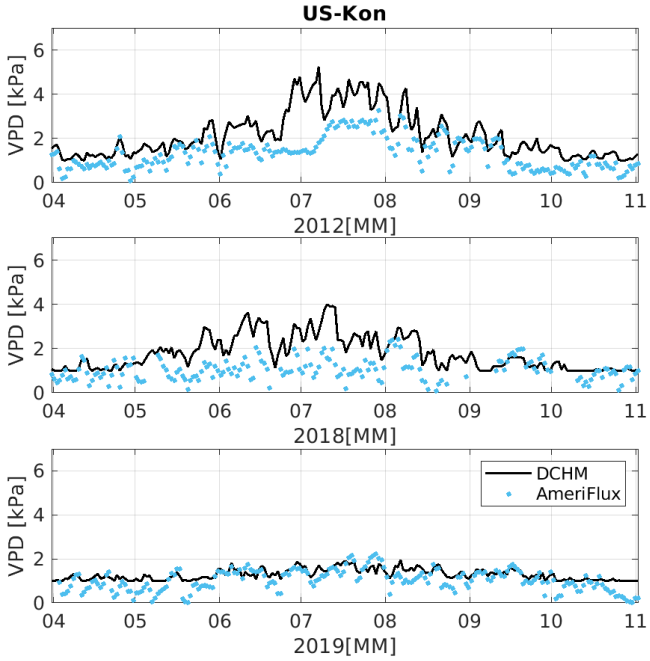

Figure S30. Daily vapor pressure deficit at US-Kon for (a) 2012 - flash drought, (b) 2018 - drought and (c) 2019 - non-drought. The DCHM computes VPD using air temperature and vapor pressure from NLDAS-2 Forcing File A.